Lithium chloride prevents glucocorticoid-induced osteonecrosis of femoral heads and strengthens mesenchymal stem cell activity in rats

Yue-Lei Zhang[1], Zhen-Zhong Zhu[2], Le-Cheng Zhang[1], Gang Wang[1]

[1]Department of Orthopedics, The First Affiliated Hospital of Anhui Medical University, Hefei, Anhui 230000, China;
[2]Department of Orthopedic Surgery, Shanghai Jiao Tong University Affiliated Sixth People's Hospital, Shanghai 200233, China.

Background: Accumulating evidence suggests that lithium influences mesenchymal stem cell (MSC) proliferation and osteogenic differentiation. As decreased bone formation in femoral heads is induced by glucocorticoids (GCs), we hypothesized that lithium has a protective effect on GC-induced osteonecrosis of femoral heads (ONFH).

Methods: A rat ONFH model was induced by methylprednisolone (MP) and the effect of lithium chloride on the models was evaluated. Micro-computed tomography (CT)-based angiography and bone scanning were performed to analyze the vessels and bone structure in the femoral heads. Hematoxylin and eosin and immunohistochemical staining were performed to evaluate the trabecular structure and osteocalcin (OCN) expression, respectively. Bone marrow-derived MSCs were isolated from the models, and their proliferative and osteogenic ability was evaluated. Western blotting and quantitative real-time polymerase chain reaction were performed to detect osteogenic-related proteins including Runx2, alkaline phosphatase, and Collagen I.

Results: Micro-CT analysis showed a high degree of osteonecrotic changes in the rats that received only MP injection. Treatment with lithium reduced this significantly in rats that received lithium (MP + Li group); while 18/20 of the femoral heads in the MP showed severe osteonecrosis, only 5/20 in the MP + Li showed mild osteonecrotic changes. The MP + Li group also displayed a higher vessel volume than the MP group (0.2193 mm^3 *vs.* 0.0811 mm^3, $P < 0.05$), shown by micro-CT-based angiography. Furthermore, histological analysis showed better trabecular structures and more OCN expression in the femoral heads of the MP + Li group compared with the MP group. The *ex vivo* investigation indicated higher proliferative and osteogenic ability and upregulated osteogenic-related proteins in MSCs extracted from rats in the MP + Li group than that in the MP group.

Conclusions: We concluded that lithium chloride has a significant protective effect on GC-induced ONFH in rats and that lithium also enhances MSC proliferation and osteogenic differentiation in rats after GC administration.

Keywords: Lithium; Osteonecrosis of femoral heads; ONFH; Bone marrow-derived mesenchymal stem cell; Proliferation; Osteogenic differentiation

Introduction

Glucocorticoid (GC) usage is the most common cause of non-traumatic osteonecrosis of the femoral heads (ONFH). Although several methods have been suggested to prevent GC-induced ONFH, no one method has attained widespread clinical use.[1-3] Mesenchymal stem cells (MSCs) are multipotent progenitors that differentiate into a variety of cell types and are the precursors of osteoblasts and osteocytes in bone tissue.[4] GC has been demonstrated to downregulate telomerase activity and accelerate the senescence of MSCs, resulting in a loss of their stem cell characteristics, including the reduced proliferative ability.[5] Furthermore, MSC differentiation into the osteogenic lineage is also inhibited by high concentrations of GC.[6] Considering the reduced bone formation induced by GC, medications that stimulate MSC activity and increase bone formation may be useful for the prevention of GC-induced ONFH.

Lithium has been used in the treatment of bipolar disorders and granulocytopenia for decades. Recent studies on this topic have demonstrated that lithium stimulates MSC proliferation, promotes osteogenic differentiation, and inhibits adipogenic differentiation of MSCs by activating the Wnt/β-catenin pathway.[7,8] Lithium also significantly enhances bone formation in rats[9] and accelerates fracture healing clinically.[10] In addition, lithium is taken up by a variety of tissues, with bone and muscle containing the highest concentrations, making lithium especially suitable for treating bone disorders.[8,11] Therefore, in this study, we investigated the effect of lithium on GC-induced ONFH and bone marrow-derived MSCs activity in ONFH models.

Access this article online

Quick Response Code:

Website: www.cmj.org

DOI: 10.1097/CM9.0000000000001530

Correspondence to: Gang Wang, Department of Orthopedics, The First Affiliated Hospital of Anhui Medical University, Hefei, Anhui 230000, China
E-Mail: orthowanggang@163.com

Chinese Medical Journal 2021;134(18)
Received: 18-09-2020 **Edited by:** Li-Shao Guo

Methods

Animal models and treatment

All procedures adhered to the recommendations of the U.S. Department of Health for the care and use of laboratory animals and were approved by the Ethics Committee of Anhui Medical University. A rat model of ONFH was induced by intramuscular injection of methylprednisolone (MP) at a dose of 30 mg/kg daily for three continuous days per week over a period of 3 weeks (nine injections in total). Thirty Sprague-Dawley rats were randomly divided into three groups. Group I was the control group ($n = 10$) and underwent no treatment, group II was the MP group ($n = 10$) in which the ONFH model was induced, and group III was the MP + Li group ($n = 10$), ONFH-modeled rats that received 0.2% lithium chloride-containing feed for 2 weeks before ONFH modeling followed by continuous feeding with lithium-containing feed until sacrifice. All the rats were specific pathogen-free (SPF) animals kept in a clean, humidity, and the temperature-controlled environment with a 12 h light/dark cycle, and free access to water and food. All samples were obtained 3 weeks after ONFH model building under anesthesia by intraperitoneal injection with 30 mg/kg pentobarbital, and all attempts were made to minimize suffering.

Angiography

Five rats in each group were used for femoral head angiography, as previously described.[12] Specifically, after successful anesthesia, the abdominal aorta was clamped, and the abdominal vein was incised. Heparinized saline, 4% paraformaldehyde, and Microfil (MV-112, Flow Tech, Inc., Carver, MA, USA) were consecutively perfused into the distal abdominal aorta until a constant flow was observed from the abdominal vein. Subsequently, the rats were stored at 4°C overnight, and the femoral heads were sampled.

Evaluation of ONFH

Both femoral heads from each rat were evaluated for bone morphological changes with micro-computed tomography (CT) scanner at a voxel of 9 μm. Next, the 2-D images were transferred into the CTVOX software (Bruker Corp., Billerica, MA, USA) to construct a 3-D image with the appropriate section. CTAn software (SkyScan; Bruker, Kontich, Belgium) was then used to evaluate the trabecular parameters of the subchondral bone in the femoral heads, including bone mineral density (BMD), bone volume (BV), bone volume per tissue volume (BV/TV), trabecular pattern factor (Tb.Pf), trabecular thickness (Tb.Th), and trabecular number (Tb.N).

To further evaluate the trabecular structure and osteocalcin (OCN) expression, hematoxylin and eosin (HE) and immunohistochemical staining were performed. In brief, after decalcification and paraffin embedding, the femoral heads were sectioned at a thickness of 5 μm in the coronal plane; next, parts of these sections were stained with HE, and other sections were deparaffinized, the antigen retrieved, and incubated with rabbit anti-rat OCN primary antibody (CST, Beverly, MA, USA) followed by incubation with a biotinylated secondary antibody. After color development with 3,3'-diaminobenzidine and counter-stained with hematoxylin, the sections were examined under a LEICA DM 4000 microscope (Leica, Wetzlar, Germany).

Evaluation of femoral head vessels

Femoral heads with angiography were decalcified and scanned with the micro-CT scanner at a voxel of 9 μm. Two-dimensional images were used to construct 3-D images of the vessels with CTVOX software. The total vessel volume in the femoral heads was analyzed with CTAn software.

Isolation of bone marrow-derived MSCs

Mesenchymal stem cells were extracted from the rats in each group, as described in the literature,[13] and were plated in T25 culture flasks and incubated in an atmosphere of 5% CO_2 at 37°C. The medium was changed every 3 days, and passages were performed when cells were 80–90% confluent. MSCs after three to five passages were used in the following *ex vivo* studies.

Proliferative activity of MSCs

Mesenchymal stem cell proliferation was evaluated with a cell counting kit-8 (CCK-8), according to the manufacturer's instructions. Specifically, MSCs from each rat were plated in 96-well plates at an initial concentration of 4000 cells/well. At indicated time points for up to 6 days, 10 μL CCK-8 was added to each well containing 100 μL culture medium and incubated for another 2 h, after which the absorbance values were measured at 450 nm. Increased cell numbers were expressed with the *D* value between the value detected at the appropriate time and the initial value measured after MSC adhesion.

The colony-forming unit (CFU) method was also used to detect the proliferative activity of MSCs. Briefly, 400 MSCs from the third passage from each rat were plated in 6-well plates and incubated in a complete medium for 10 days; next, the medium was discarded, the cells were fixed with 4% paraformaldehyde for 20 min and stained with 0.2% crystal violet dye for 30 min. A cell mass that contained > 50 cells was described as a colony.

Osteogenic induction

To detect the osteogenic differentiation ability of MSCs in the rats of each group, cells were incubated in an osteogenic induction medium consisting of the complete medium supplemented with 10^{-2} mol/L β-sodium glycerophosphate, 50 μg/mL L-ascorbic acid, and 10^{-7} mol/L dexamethasone. The medium was changed every 3 days until assessment at the indicated time.

Alkaline phosphatase (ALP) activity and ALP staining assay

Mesenchymal stem cells were plated in 12-well plates and incubated in an osteogenic induction medium for 1 week,

after which the cells were lysed with 0.2% Triton-X, centrifuged at 12,000 r/min for 15 min, and the ALP activity in the supernatant measured with an ALP activity assay (Nanjing Jiancheng Bioengineering Institute, Nanjing, China), according to the manufacturer's instructions. Absorbances were measured at 520 nm and normalized to protein concentrations detected by a BCA kit (Thermo Fisher Scientific, Rockford, IL, USA).

Mesenchymal stem cells differentiated for 1 week were fixed with 4% paraformaldehyde and stained with the 5-Bromo-4-chloro-3-indolyl phosphate/nitro blue tetrazolium Alkaline Phosphatase Color Development Kit (Beyotime, Shanghai, China), according to the manufacturer's instructions.

Alizarin red S staining

After osteogenic induction for 14 days, the medium was discarded. MSCs were rinsed with phosphate-buffered saline (PBS), stained with 2% alizarin red S working solution for 30 min, and washed again with PBS three times. The alizarin red stain was observed with an inverted phase-contrast microscope.

Western blotting

To detect the osteogenic-related protein expression in the MSCs in each group, cells were incubated in an osteogenic induction medium for 1 week. Total protein was then extracted with cell lysis buffer and measured with a BCA kit (Thermo Scientific). Then, 40 μg total protein was separated on 10% sodium dodecyl sulfate (SDS)-polyacrylamide gel electrophoresis (PAGE) gels and transferred onto polyvinylidene difluoride membranes; after blocking with 5% non-fat dry milk, the membranes were incubated overnight at 4°C with the following primary antibodies: anti-Runx2 antibody (Abcam, Cambridge, CA, USA), anti-Collagen I antibody (CST, Beverly, MA, USA), and anti-GAPDH antibody (CST, Beverly, MA, USA). All the antibodies were rabbit monoclonals and were diluted 1:1000 upon use. After rinsing with PBS, the membranes were incubated with horseradish peroxidase (HRP)-conjugated secondary anti-rabbit antibody (CST, Beverly, MA, USA) at 1:2000 dilution for 1 h at 37°C. After rinsing again, the membrane was scanned in an Odyssey Scanner (Li-COR Biosciences, Lincoln, NE, USA).

Quantitative reverse-transcription polymerase chain reaction

Total RNA was extracted from osteogenic-induced MSCs using a TRIzol method, and 1 μg RNA was converted to cDNA with EasyScript One-Step gDNA Removal and cDNA Synthesis Supermix (TransGen Biotech, Beijing, China). Next, polymerase chain reaction (PCR) was performed using the TransStart Tip Green qPCR SuperMix method (TransGen, Beijing, China) with 1 μL cDNA, and real-time quantification was performed on ABI Prism 7900 (Invitrogen, Waltham, MA, USA). The reaction conditions were as follows: 95°C for 30 s, followed by 40 cycles of 95°C for 5 s and 60°C for 30 s. The primer sequences of each cDNA were as follows: GTCATCCATGGCGAACTGGT-3 and CGTCATCCATGGCGAACTGG for *β-actin*, CCGAGACCAACCGAGTCATTTA and AAGAGGCTGTTTGACGCCAT for *Runx2*, CACATGCCGTGACCTCAAGA and TCGATCCAGTACTCTCCGCT for *Collagen I*, and CAAGGATGCTGGGAAGTCCG and CTCTGGGCGCATCTCATTGT for *ALP*. *β-actin* was used as a control. The relative expression of mRNA was calculated by the fold change method.

Statistical analysis

All data are presented as mean ± standard deviations (SD). Comparisons between groups were performed using one-way analysis of variance with Tukey's *post hoc* test, and $P < 0.05$ was designated as the level of statistical difference between groups.

Results

Effect of lithium on the occurrence of ONFH and the microstructures of femoral heads in rats with MP injection

To investigate the effect of lithium on MP-induced ONFH, micro-CT scanning was performed to evaluate the bone tissue in the femoral heads. The results showed that 18 femoral heads of the rats that received only long-term MP injection exhibited significant trabecular changes, such as bone mineral loss and cystic degeneration in the subchondral area, compared with the normal rats. In contrast, only five femoral heads in the MP + Li group showed mild osteonecrotic changes with ameliorated deteriorations in the subchondral area Moreover, the trabecular parameters in the femoral heads, including BMD, BV, BV/TV, Tb.Th, and Tb.N, which reflect the trabecular structure, were also analyzed statistically. Significantly higher values of these parameters were observed in rats of the MP + Li group than in the MP group, although the values were not higher than those of the control group. Tb.Pf is a parameter that represents a continuity of the bone trabeculae with lower Tb.Pf values indicating better trabecular continuity. Micro-CT analysis showed lower Tb.Pf values in rats with MP + Li administration compared with rats with MP administration only, indicating better trabecular structure when lithium was used accompanied by MP treatment. However, the trabecular structures of the femoral heads in the MP + Li group were still poorer than those in the control group [Figure 1].

Hematoxylin and eosin staining was performed to further evaluate the microstructures of the femoral heads from each group. We observed complete ossification in the subchondral area of the femoral heads in the control group, indicating that the sample time point was appropriate to analyze the effects of MP and lithium. The femoral heads in the MP group showed either no trabecular structures or large areas of necrotic tissue with a few sparse trabecular structures (the latter is shown in Figure 2A). In contrast, in the MP + Li group, the trabecular structure was good and only small amounts of trabecular structure and bone marrow were replaced by necrotic tissue [Figure 2A and 2B]. Further investigation showed that the necrotic areas in both the MP and MP + Li

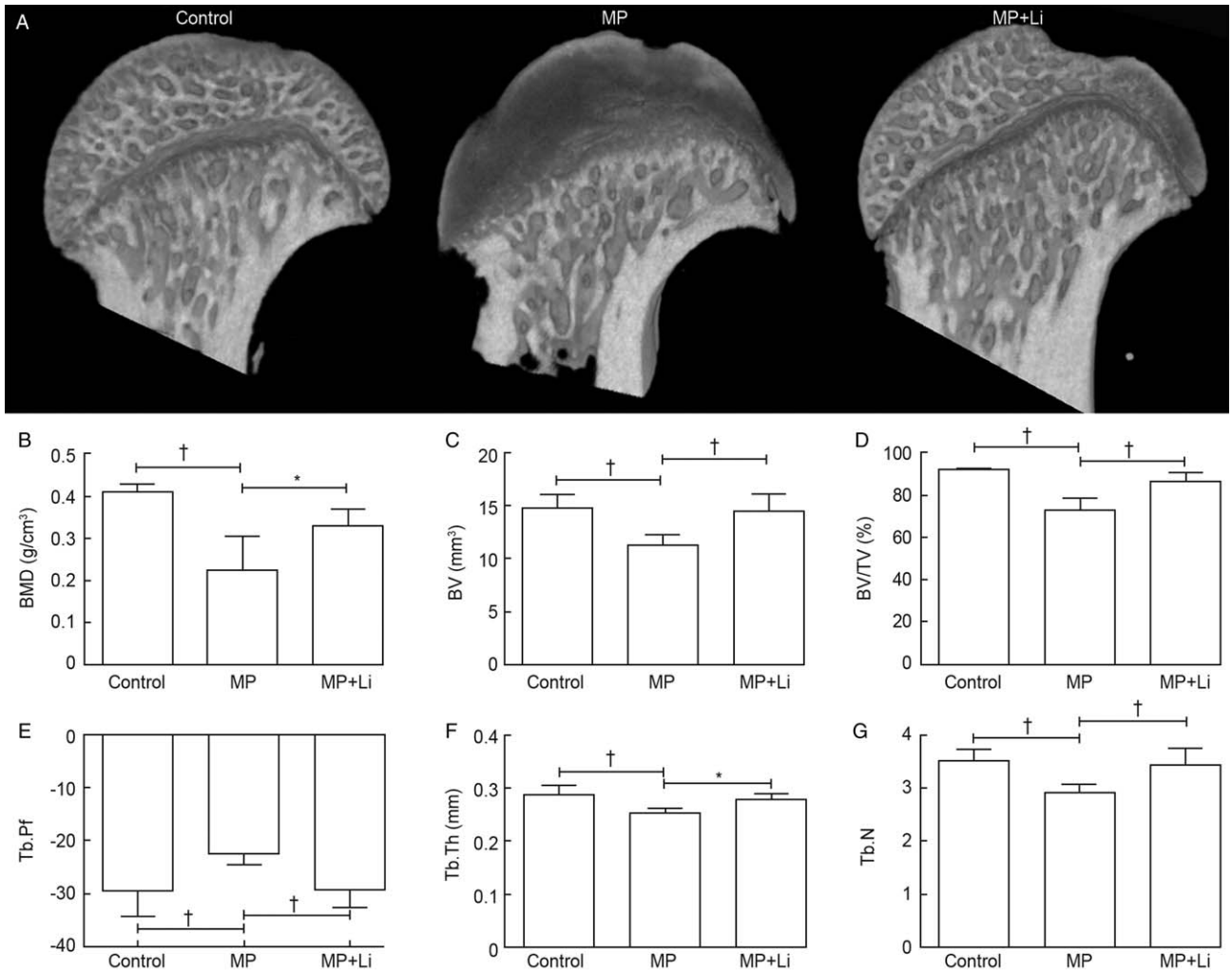

Figure 1: Micro-CT analysis of femoral heads from each group. (A) Representative 3-D images of femoral heads at the coronal section of each group. (B–G) Analysis of trabecular parameters, including BMD, BV, BV/TV, Tb.Th, Tb.N, and Tb.Pf. $^{*}P < 0.05$, $^{+}P < 0.01$. BMD: Bone mineral density; BV/TV: Bone volume per tissue volume; BV: Bone volume; CT: Computed tomography; Tb.N: Trabecular number; Tb.Pf: Trabecular pattern factor; Tb.Th: Trabecular thickness.

groups were filled with many non-structural chondrocytes [Figure 2B]. Moreover, we detected OCN expression in these femoral heads. The results showed the presence of large brown-staining areas in the trabeculae of rats with vehicle treatment; there was almost no OCN expression in the necrotic areas in the MP group, and greater numbers of these brown-staining areas were observed in femoral heads from the MP + Li group than from the MP group [Figure 2C].

Effect of lithium on the femoral head blood supply in rats with MP injection

The blood infusion in femoral heads was evaluated by angiography with Microfil. The results showed significantly decreased numbers of blood vessels in rats with ONFH and slightly fewer blood vessels in rats without ONFH in the MP group, especially in the subchondral area above the epiphyseal line. However, there were more vessels present even in femoral heads with osteonecrosis in the MP + Li group than in the MP group [Figure 3]. Statistical analysis indicated similar results with angiography. The total blood vessel volume in femoral heads was clearly lower in the MP group than that in both the control and MP + Li groups.

Effect of lithium on MSC proliferative ability in rats with MP injection

MSCs extracted from rats of each group were evaluated and the total cell numbers at each time point were determined with a proliferation kit. The total MSC numbers in each group increased dramatically within 6 days and differed from each other after 4 days of culture. The absorbance values in the MP group were significantly lower than those in the control group, and the cell numbers extracted from rats in the MP + Li group were clearly higher than those in the MP group at the fourth and sixth day of culture [Figure 4A].

Colony-forming unit is an additional index of proliferative ability. We observed fewer colonies in MSCs extracted

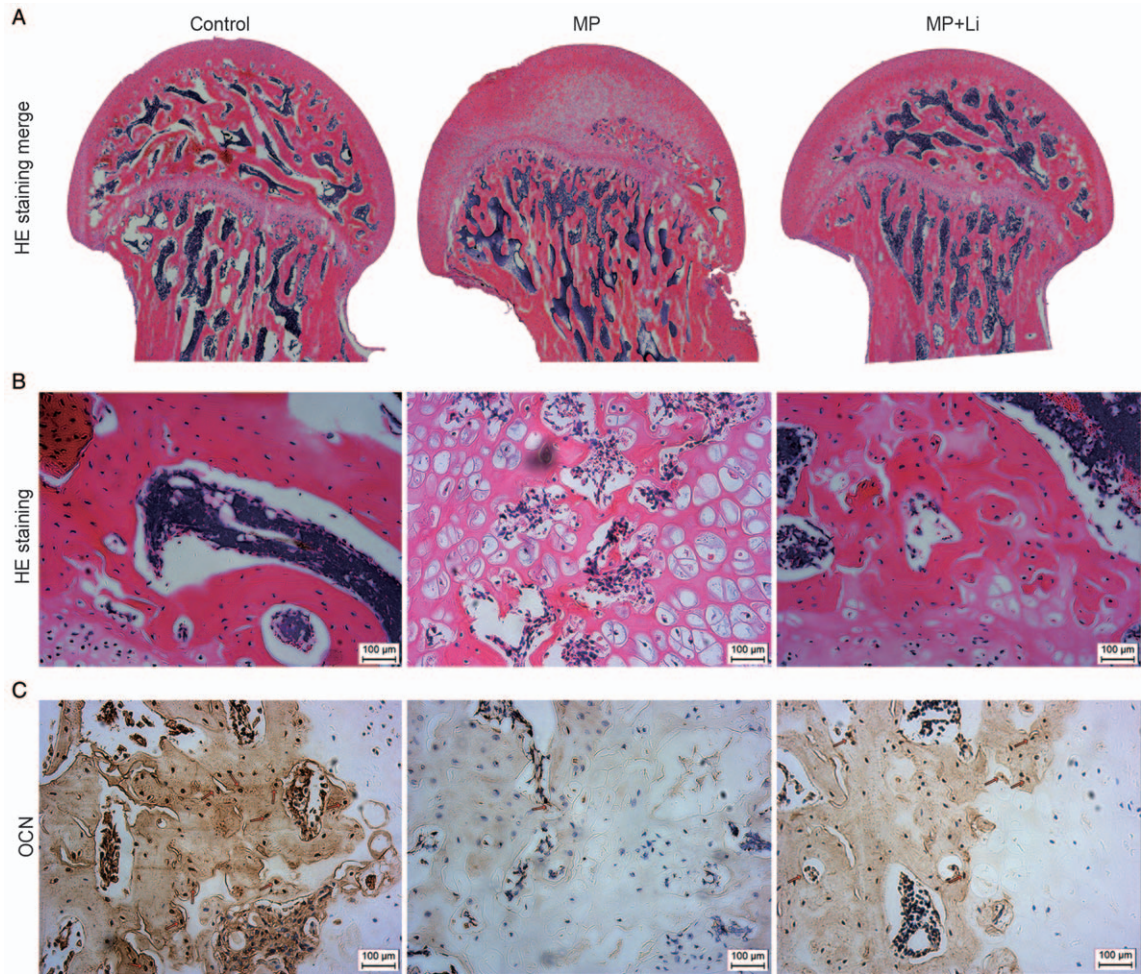

Figure 2: Histological analysis of femoral heads from each group. (A) Representative merged HE-stained images show the coronal sections of femoral heads from each group (Original magnification × 5). (B) Representative magnification of HE-stained femoral head slices in each group, the necrotic area was occupied by many non-structural chondrocytes. (C) Representative immunohistochemical images of OCN in each group. Arrows indicate OCN-positive osteocytes. HE: Hematoxylin and eosin; Li: Lithium; MP: Methylprednisolone; OCN: Osteocalcin. Bar = 100 μm.

from MP-treated rats than in the control and more colonies in the group treated with MP + Li than in the MP group after initial plating with the same numbers of MSCs [Figures 4B and 4C].

Effect of lithium on MSC osteogenic differentiation in rats with MP injection

Alkaline phosphatase was shown to be a late osteogenic marker of MSCs. We observed that MSCs extracted from the ONFH model induced by MP showed significantly less ALP staining than cells in the control group after osteogenic induction for 1 week while more ALP-staining cells were observed in MSCs extracted from rats with MP + Li treatment than in the MP group [Figure 5A]. Further investigation of ALP activity showed that MSCs from the MP + Li treated rats had greater ALP protein expression (nearly fourfold) than those from MP-treated rats, although less than the control group [Figure 5C]. Further alizarin red staining showed fewer calcium deposits in MSCs of the MP group than in the control, indicating that MP injection significantly damaged the osteogenic differentiation ability of MSCs in rats. Similarly, there were more red-stained calcium nodules in MSCs extracted from MP + Li-treated rats than from MP-treated rats [Figure 5B].

Runx2 protein, the most important transcriptional factor involved in MSCs osteogenic differentiation, was also analyzed with western blotting analysis. The levels of Runx2 protein in MSCs were significantly downregulated by *in vivo* use of MP, and supplementation of lithium enhanced Runx2 expression in MSCs. Collagen type I, another protein involved in MSC osteogenic differentiation, was also detected. The results showed that MSC in the rats of the MP group had less collagen type I expression than those in the control group, and denser bands were present in MSC lysates from the MP + Li-treated rats compared with the MP group [Figure 5D]. Furthermore, we detected osteogenic-related mRNA (Runx2, ALP, and collagen I) expression in osteogenic-induced MSCs from each group. Similarly, the mRNA expression, especially that of Runx2, was higher in MP + Li-treated rats than that in rats treated only with MP [Figures 5E–G].

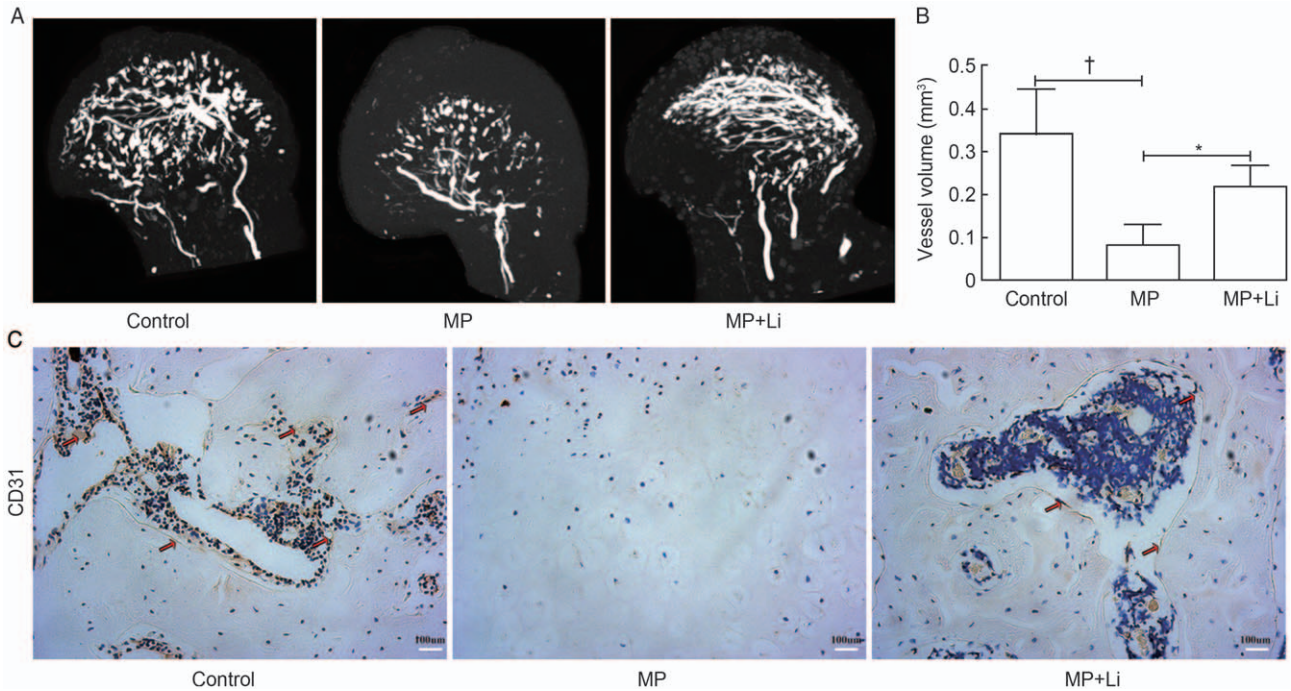

Figure 3: Angiography analysis of femoral heads. (A) Representative 3-D images of blood vessels in femoral heads. Blood vessels are labeled with white color. (B) Total vessel volume analysis of femoral heads from each group. $^{*}P < 0.05$, $^{+}P < 0.01$. (C) Representative images of CD31 staining in the femoral heads of each group. The arrow indicates a CD31-positive endothelial cell. Bar = 100 mm. Li: Lithium; MP: Methylprednisolone.

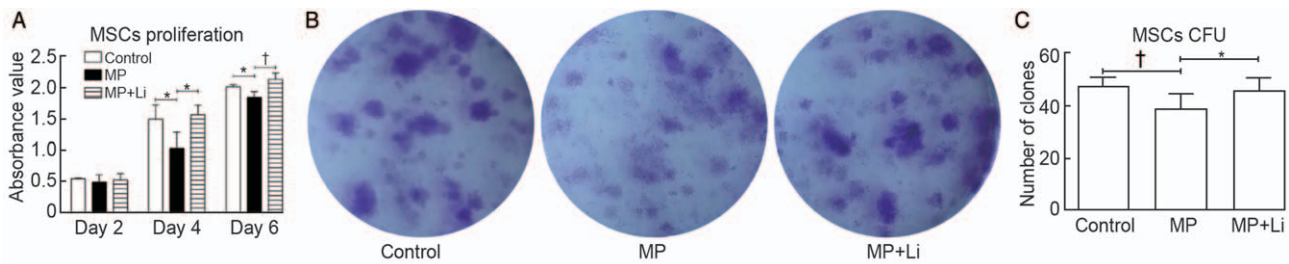

Figure 4: Evaluation of the proliferative ability of MSCs extracted from rats from each group. (A) MSCs proliferation detected with CCK-8. D values between the absorbance values detected at the appropriate time and the initial values measured after MSC adhesion were analyzed ($n = 5$, $^{*}P < 0.05$, $^{+}P < 0.01$). (B) Representative CFU images of MSCs stained with crystal violet from each group. (C) Statistical analysis of colony numbers in each group ($n = 5$, $^{*}P < 0.05$, $^{+}P < 0.01$). CCK-8: Cell counting kit-8; CFU: Colony-forming unit; Li: Lithium; MP: Methylprednisolone; MSCs: Mesenchymal stem cells.

Discussion

Lithium chloride, which has been used in clinical treatments for many years, has recently become a research focus for bone metabolism. Zhu *et al*[8] reported that lithium stimulated human bone marrow-derived MSC proliferation at a concentration of 5 mmol/L through GSK3β-mediated canonical Wnt pathway activation. Tang *et al*[7] demonstrated that lithium effectively promoted osteogenesis and inhibited adipogenesis in bone marrow-derived MSCs by simultaneously influencing the Wnt and Hh pathways. Hu *et al*[14] further concluded that lithium inhibited osteoclastogenesis and osteoclastic bone resorption by inhibiting the nuclear factor-kappa B (NF-κB) Ligand (RANKL)-induced NF-κB signaling pathway. All these studies showed that lithium has a positive effect on bone metabolic disease. Similar to the protective effects observed in GC-mediated neural progenitor cells,[15,16] lithium was observed to rescue the abnormal osteoblast/adipocyte balance of MSCs in dexamethasone-treated mice[17] and rats with GC-induced ONFH[18] through Wnt/beta-catenin pathway activation. Furthermore, a composite scaffold containing lithium improved the viability of GC-treated MSCs and vascular endothelial cells, as well as increasing the expression of osteogenic and angiogenic factors *in vitro* and improving new bone formation in GC-treated rabbits.[19] In this study, we observed that lithium chloride could prevent GC-induced ONFH in rats, as previously reported.[20] Furthermore, the bone marrow-derived MSC activity, including proliferation and differentiation, in rats with ONFH was enhanced by lithium treatment. These results indicated that lithium may be a promising medication to accompany GC therapy for the clinical prevention of ONFH.

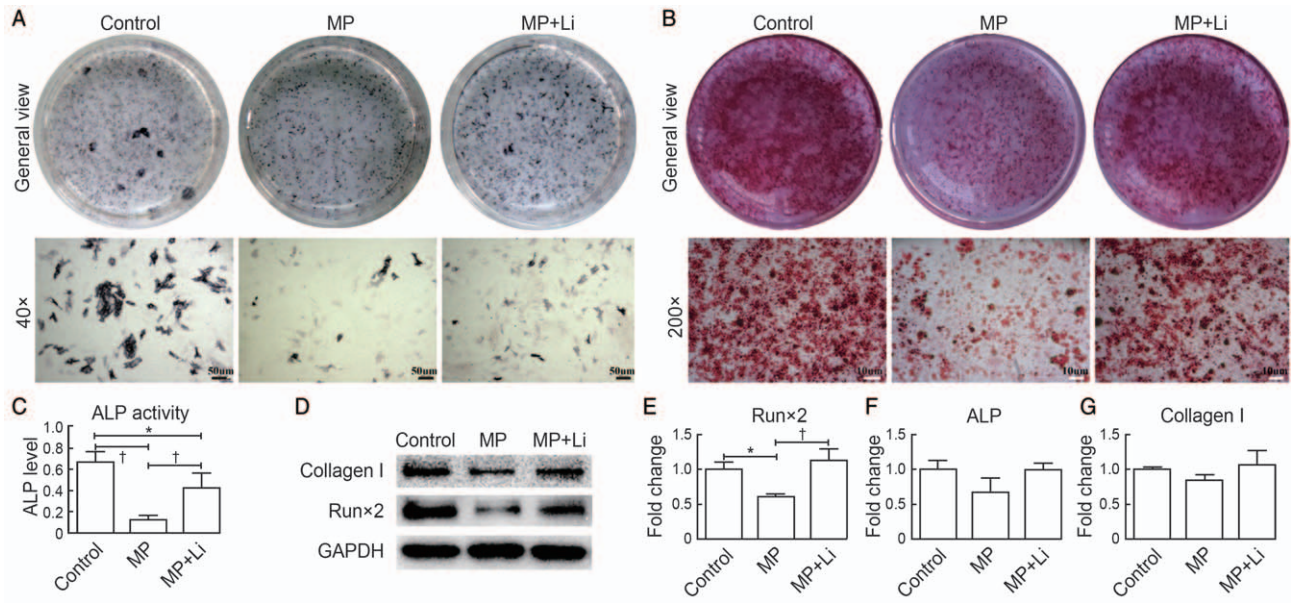

Figure 5: Osteogenic differentiation analysis of MSCs extracted from rats in each group. (A) General and magnification images of ALP-stained MSCs after osteogenic induction for 1 week (Original magnification × 40). (B) General and magnification (Original magnification × 200) images of alizarin red S-stained MSCs after osteogenic induction for 2 weeks. (C) ALP activity in MSCs after osteogenic induction for 1 week ($n = 5$, $^{*}P < 0.05$, $^{+}P < 0.01$). (D) Western blotting analysis of Runx2 and Collagen I proteins in MSCs incubated in osteogenic induction medium for 1 week; GAPDH represents as the control. (E–G) Runx2, ALP, and Collagen I mRNA analysis with qRT-PCR (each in triplicate, $^{*}P < 0.05$, $^{+}P < 0.01$). ALP: Alkaline phosphatase; Li: Lithium; MP: Methylprednisolone; MSCs: Mesenchymal stem cells; qRT-PCR: Quantitative reverse transcription-polymerase chain reaction.

Osteonecrosis of femoral heads usually presents radiographically as a loss of subchondral trabecular and histologically as a replacement of trabecular by necrotic tissue,[21] which is similar to our observations. In this study, the rats with GC administration had almost invisible structural trabeculae and decreased BV and BMD in the subchondral bone. Further histological study showed that the necrotic area was occupied by non-structural chondrocytes, which is consistent with the findings of several studies,[22,23] but differs from others that showed large numbers of empty lacunae filling the bone trabeculae, as well as disordered, sparser, or destroyed bone trabeculae.[24,25] Since Morini *et al*[26] observed that subchondral trabeculae originated from the ossification of the diaphysis and do not start before the third month, we speculate that the differences in the histological studies were likely due to different treatments and different sampling times. In addition, the rats that received GC treatment accompanied by lithium presented with fewer pathological changes and relatively normal trabecular structures, together with better trabecular parameters, indicating the protective effect of lithium against bone loss in femoral heads induced by GC.

The blood supply of the femoral head is seriously damaged by GCs,[27] which is consistent with our findings. Furthermore, we also observed that lithium ameliorated the blood vessel injury induced by GC and promoted angiogenesis. This is represented by CD31 accompaniment of the decreased bone loss in the femoral head, which may contribute to the coupling of angiogenesis and osteogenesis. Endothelial cells could enhance osteogenic differentiation of MSCs *via* direct cell–cell contact and, conversely, growth of the vascular network is also regulated by signals provided by bone cells.[28,29] Moreover, the effect of lithium on vessels has been confirmed by several studies. Birdsey *et al*[30] observed that lithium corrected vessel defects in embryos with endothelial deletion of ERG. Furthermore, Saghiri *et al*[31] concluded that lithium upregulated vasculogenesis by inducing the expression of matrix metalloproteinase (MMP)-9 and vascular endothelial growth factor (VEGF) through activation of the Wnt/β-catenin pathway in their review. These results showed that the influence on blood supply may be another important effect in lithium's prevention of GC-induced ONFH. However, vascularization in the femoral head of the rat differs from that in the human.[26] In humans, the femoral heads are fed mainly by the epiphyseal arterial network formed by branches of the retinacular arteries above the epiphyseal scar,[32] while in the rat, the vascularization of the femoral head arises from the diaphyseal vasculature, penetrated from the metaphysis into the epiphyseal cartilage and extended widely into the femoral head,[26] consistent with our angiographic studies. Therefore, whether the angiographic findings using this rat model can be directly transferred to the human situation requires further study.

Mesenchymal stem cells are progenitors of osteogenic cell lines, and decreased MSC activity has been considered a mechanism of GC-induced ONFH. Studies have demonstrated that GCs inhibit MSC capabilities including proliferation and differentiation *in vitro* and *in vivo*,[6,33,34] which corresponds to our *ex vivo* study. Here, we observed that bone marrow-derived MSCs extracted from GC-treated rats presented both reduced proliferative and osteogenic ability, indicating that reduced MSC capability played a critical role in the low repair capacity of GC-induced ONFH and may be sustained for a long time even after GC withdrawal. Meanwhile, we

observed that MSCs from lithium-treated rats showed stronger proliferative and osteogenic ability than those treated only with GC, which is similar to the findings of several studies that showed that lithium promoted proliferation and stimulated osteogenic differentiation of MSCs in *in vitro* cultures,[7,8,35] suggesting that lithium prevented bone loss in femoral heads probably through the protective effect on MSCs.

Lithium has been considered to be an activator of Wnt/β-catenin signaling by suppressing GSK-3β, a kinase which constitutively phosphorylates β-catenin, leading to the degradation of β-catenin by the proteasome.[36] Studies have demonstrated that[37] GC excess exerted its detrimental effect on bone formation partially due to inhibition of Wnt-signaling, and that activation of Wnt/β-catenin signaling significantly stimulated proliferation and osteogenesis in mesenchymal cells.[8,38] We, therefore, speculate that the effects of lithium on GC-treated rats may have contributed to the activation of Wnt/β-catenin signaling, although no further detection of this pathway in this study. However, further study on the mechanism of lithium in bone metabolism will be undertaken both *in vivo* and *in vitro*.

Conclusions

Our findings demonstrate that lithium chloride exerts prominent protective effects against GC-induced ONFH in rats. Further investigations on bone marrow-derived MSCs extracted from these rats confirmed that lithium enhances both MSC proliferation and osteogenic differentiation in rats after GC administration.

Funding

This study was supported by a grant from the National Natural Science Foundation of China (No. 81702134).

Conflicts of interest

None.

References

1. Zhang YL, Yin JH, Ding H, Zhang W, Zhang CQ, Gao YS. Vitamin K2 prevents glucocorticoid-induced osteonecrosis of the femoral head in rats. Int J Biol Sci 2016;12:347–358. doi: 10.7150/ijbs.13269.
2. Ding Z, Shi H, Yang W. Osteoprotective effect of cimiracemate in glucocorticoid-induced osteoporosis by osteoprotegerin/receptor activator of nuclear factor kappa B/receptor activator of nuclear factor kappa-beta ligand signaling. Pharmacology 2019;103:163–172. doi: 10.1159/000495509.
3. Kuang MJ, Huang Y, Zhao XG, Zhang R, Ma JX, Wang DC, *et al*. Exosomes derived from Wharton's jelly of human umbilical cord mesenchymal stem cells reduce osteocyte apoptosis in glucocorticoid-induced osteonecrosis of the femoral head in rats via the miR-21-PTEN-AKT signalling pathway. Int J Biol Sci 2019;15:1861–1871. doi: 10.7150/ijbs.32262.
4. Garg P, Mazur MM, Buck AC, Wandtke ME, Liu J, Ebraheim NA. Prospective review of mesenchymal stem cells differentiation into osteoblasts. Orthop Surg 2017;9:13–19. doi: 10.1111/os.12304.
5. Wei N, Yu Y, Schmidt T, Stanford C, Hong L. Effects of glucocorticoid receptor antagonist, RU486, on the proliferative and differentiation capabilities of bone marrow mesenchymal stromal cells in ovariectomized rats. J Orthop Res 2013;31:760–767. doi: 10.1002/jor.22298.
6. Koromila T, Baniwal SK, Song YS, Martin A, Xiong J, Frenkel B. Glucocorticoids antagonize RUNX2 during osteoblast differentiation in cultures of ST2 pluripotent mesenchymal cells. J Cell Biochem 2014;115:27–33. doi: 10.1002/jcb.24646.
7. Tang L, Chen Y, Pei F, Zhang H. Lithium chloride modulates adipogenesis and osteogenesis of human bone marrow-derived mesenchymal stem cells. Cell Physiol Biochem 2015;37:143–152. doi: 10.1159/000430340.
8. Zhu Z, Yin J, Guan J, Hu B, Niu X, Jin D, *et al*. Lithium stimulates human bone marrow derived mesenchymal stem cell proliferation through GSK-3beta-dependent beta-catenin/Wnt pathway activation. FEBS J 2014;281:5371–5389. doi: 10.1111/febs.13081.
9. Pan J, He S, Yin X, Li Y, Zhou C, Zou S. Lithium enhances alveolar bone formation during orthodontic retention in rats. Orthod Craniofac Res 2017;20:146–151. doi: 10.1111/ocr.12190.
10. Vachhani K, Whyne C, Wang Y, Burns DM, Nam D. Low-dose lithium regimen enhances endochondral fracture healing in osteoporotic rodent bone. J Orthop Res 2018;36:1783–1789. doi: 10.1002/jor.23799.
11. Kurgan N, Bott KN, Helmeczi WE, Roy BD, Brindle ID, Klentrou P, *et al*. Low dose lithium supplementation activates Wnt/beta-catenin signalling and increases bone OPG/RANKL ratio in mice. Biochem Biophys Res Commun 2019;511:394–397. doi: 10.1016/j.bbrc.2019.02.066.
12. Ding H, Gao YS, Wang Y, Hu C, Sun Y, Zhang C. Dimethyloxaloylglycine increases the bone healing capacity of adipose-derived stem cells by promoting osteogenic differentiation and angiogenic potential. Stem Cells Dev 2014;23:990–1000. doi: 10.1089/scd.2013.0486.
13. Boregowda SV, Krishnappa V, Phinney DG. Isolation of mouse bone marrow mesenchymal stem cells. Methods Mol Biol 2016;1416:205–223. doi: 10.1007/978-1-4939-3584-0_11.
14. Hu X, Wang Z, Shi J, Guo X, Wang L, Ping Z, *et al*. Lithium chloride inhibits titanium particle-induced osteoclastogenesis by inhibiting the NF-(B pathway. Oncotarget 2017;8:83949–83961. doi: 10.18632/oncotarget.20000.
15. Cabrera O, Dougherty J, Singh S, Swiney BS, Farber NB, Noguchi KK. Lithium protects against glucocorticoid induced neural progenitor cell apoptosis in the developing cerebellum. Brain Res 2014;1545:54–63. doi: 10.1016/j.brainres.2013.12.014.
16. Boku S, Nakagawa S, Masuda T, Nishikawa H, Kato A, Kitaichi Y, *et al*. Glucocorticoids and lithium reciprocally regulate the proliferation of adult dentate gyrus-derived neural precursor cells through GSK-3beta and beta-catenin/TCF pathway. Neuropsychopharmacology 2009;34:805–815. doi: 10.1038/npp.2008.198.
17. Li J, Zhang N, Huang X, Xu J, Fernandes JC, Dai K, *et al*. Dexamethasone shifts bone marrow stromal cells from osteoblasts to adipocytes by C/EBPalpha promoter methylation. Cell Death Dis 2013;4:e832. doi: 10.1038/cddis.2013.348.
18. Yu Z, Fan L, Li J, Ge Z, Dang X, Wang K. Lithium chloride attenuates the abnormal osteogenic/adipogenic differentiation of bone marrow-derived mesenchymal stem cells obtained from rats with steroid-related osteonecrosis by activating the β-catenin pathway. Int J Mol Med 2015;36:1264–1272. doi: 10.3892/ijmm.2015.2340.
19. Li D, Xie X, Yang Z, Wang C, Wei Z, Kang P. Enhanced bone defect repairing effects in glucocorticoid-induced osteonecrosis of the femoral head using a porous nano-lithium-hydroxyapatite/gelatin microsphere/erythropoietin composite scaffold. Biomater Sci 2018;6:519–537. doi: 10.1039/c7bm00975e.
20. Yu Z, Fan L, Li J, Ge Z, Dang X, Wang K. Lithium prevents rat steroid-related osteonecrosis of the femoral head by (-catenin activation. Endocrine 2016;52:380–390. doi: 10.1007/s12020-015-0747-y.
21. Weinstein RS. Glucocorticoid-induced osteonecrosis. Endocrine 2012;41:183–190. doi: 10.1007/s12020-011-9580-0.
22. Guo YJ, Luo SH, Tang MJ, Zhou ZB, Yin JH, Gao YS, *et al*. Muscone exerts protective roles on alcohol-induced osteonecrosis of the femoral head. Biomed Pharmacother 2018;97:825–832. doi: 10.1016/j.biopha.2017.11.025.
23. Zuo R, Kong L, Wang M, Wang W, Xu J, Chai Y, *et al*. Exosomes derived from human CD34(+) stem cells transfected with miR-26a prevent glucocorticoid-induced osteonecrosis of the femoral head by promoting angiogenesis and osteogenesis. Stem Cell Res Ther 2019;10:321. doi: 10.1186/s13287-019-1426-3.

24. Zhao X, Alqwbani M, Luo Y, Chen C, Ge A, Wei Y, *et al*. Glucocorticoids decreased Cx43 expression in osteonecrosis of femoral head: The effect on proliferation and osteogenic differentiation of rat BMSCs. J Cell Mol Med 2021;25:484–498. doi: 10.1111/jcmm.16103.
25. Peng P, Nie Z, Sun F, Peng H. Glucocorticoids induce femoral head necrosis in rats through the ROS/JNK/c-Jun pathway. FEBS Open Bio 2020;11:312–321. doi: 10.1002/2211-5463.13037.
26. Morini S, Pannarale L, Franchitto A, Donati S, Gaudio E. Microvascular features and ossification process in the femoral head of growing rats. J Anat 1999;195:225–233. doi: 10.1046/j.1469-7580.1999.19520225.x.
27. Zhang Y, Yin J, Ding H, Zhang C, Gao YS. Vitamin K2 ameliorates damage of blood vessels by glucocorticoid: A potential mechanism for its protective effects in glucocorticoid-induced osteonecrosis of the femoral head in a rat model. Int J Biol Sci 2016;12:776–785. doi: 10.7150/ijbs.15248.
28. Kusumbe AP, Ramasamy SK, Adams RH. Coupling of angiogenesis and osteogenesis by a specific vessel subtype in bone. Nature 2014;507:323–328. doi: 10.1038/nature13145.
29. Rumney RMH, Lanham SA, Kanczler JM, Kao AP. In vivo delivery of VEGF RNA and protein to increase osteogenesis and intraosseous angiogenesis. Sci Rep 2019;9:17745. doi: 10.1038/s41598-019-53249-4.
30. Birdsey GM, Shah AV, Dufton N, Reynolds LE, Osuna Almagro L, Yang Y, *et al*. The endothelial transcription factor ERG promotes vascular stability and growth through Wnt/beta-catenin signaling. Dev Cell 2015;32:82–96. doi: 10.1016/j.devcel.2014.11.016.
31. Saghiri MA, Orangi J, Asatourian A, Sorenson CM, Sheibani N. Functional role of inorganic trace elements in angiogenesis part III: (Ti, Li, Ce, As, Hg, Va, Nb and Pb). Crit Rev Oncol Hematol 2015;98:290–301. doi: 10.1016/j.critrevonc.2015.10.004.
32. Zhao D, Qiu X, Wang B, Wang Z, Wang W, Ouyang J, *et al*. Epiphyseal arterial network and inferior retinacular artery seem critical to femoral head perfusion in adults with femoral neck fractures. Clin Orthop Relat Res 2017;475:2011–2023. doi: 10.1007/s11999-017-5318-5.
33. Caffarini M, Armeni T, Pellegrino P, Cianfruglia L, Martino M, Offidani A, *et al*. Cushing syndrome: The role of MSCs in wound healing, immunosuppression, comorbidities, and antioxidant imbalance. Front Cell Dev Biol 2019;7:227. doi: 10.3389/fcell.2019.00227.
34. Ma L, Feng X, Wang K, Song Y, Luo R, Yang C. Dexamethasone promotes mesenchymal stem cell apoptosis and inhibits osteogenesis by disrupting mitochondrial dynamics. FEBS Open Bio 2019;10:211–220. doi: 10.1002/2211-5463.12771.
35. Satija NK, Sharma D, Afrin F, Tripathi RP, Gangenahalli G. High throughput transcriptome profiling of lithium stimulated human mesenchymal stem cells reveals priming towards osteoblastic lineage. PloS One 2013;8:e55769. doi: 10.1371/journal.pone.0055769.
36. Du Y, Ling J, Wei X, Ning Y, Xie N, Gu H, *et al*. Wnt/(-catenin signaling participates in cementoblast/osteoblast differentiation of dental follicle cells. Connect Tissue Res 2012;53:390–397. doi: 10.3109/03008207.2012.668980.
37. Meszaros K, Patocs A. Glucocorticoids influencing Wnt/(-catenin pathway; multiple sites, heterogeneous effects. Molecules 2020;25:1489. doi: 10.3390/molecules25071489.
38. Hong G, He X, Shen Y, Chen X, Yang F, Yang P, *et al*. Chrysosplenetin promotes osteoblastogenesis of bone marrow stromal cells via Wnt/(-catenin pathway and enhances osteogenesis in estrogen deficiency-induced bone loss. Stem Cell Res Ther 2019;10:277. doi: 10.1186/s13287-019-1375-x.

How to cite this article: Zhang YL, Zhu ZZ, Zhang LC, Wang G. Lithium chloride prevents glucocorticoid-induced osteonecrosis of femoral heads and strengthens mesenchymal stem cell activity in rats. Chin Med J 2021;134:2214–2222. doi: 10.1097/CM9.0000000000001530